*Journal of The Electrochemical Society*, **155** (11) J321-J325 (2008)
0013-4651/2008/155(11)/J321/5/$23.00 © The Electrochemical Society



# Pentacene Patterning on Aluminum Nitride by Water Dipping

**Hsiao-Wen Zan,[a,b,z] Cheng-Wei Chou,[a] Chung-Hwa Wang,[c] Kuo-Hsi Yen,[a] and Jenn-Chang Hwang[c]**

[a]*Department of Photonics and Institute of Electro-Optical Engineering and* [b]*Department of Photonics and Display Institute, National Chiao Tung University, 300 HsinChu, Taiwan*
[c]*Department of Materials Science and Engineering, National Tsing Hua University, HsinChu, Taiwan*

This study reports a pentacene patterning method that can be combined with conventional lithography to pattern pentacene film. The aluminum nitride (AlN) surface was patterned using a conventional photolithography process and then treated with oxygen ($O_2$) plasma on uncovered AlN to modify surface polarity. Following pentacene deposition, the sample was dipped in water to remove pentacene from the $O_2$ plasma-treated area. The $O_2$ plasma-treated AlN surface was analyzed using X-ray photoelectron spectroscopy (XPS) before pentacene deposition. The polar surface energy changed from 13.2 to 114.4 mJ/m$^2$ when the AlN surface was treated with $O_2$ plasma at 100 W for 10 min. The polar surface energy was attributed to the increase of Al–O bonds on the surface based on XPS measurements. The intrusion energy of water was enhanced from 34.5 to 140.4 mJ/m$^2$ due to the polar surface energy induced by the $O_2$ plasma treatment. The enhancement of water intrusion energy and the polar surface energy explains the water-removable pentacene patterning mechanism.
 [DOI: 10.1149/1.2976894] 

Manuscript submitted June 16, 2008; revised manuscript received July 24, 2008. Published September 22, 2008.

Organic thin-film transistors (OTFTs) have been proposed for various applications such as displays and flexible electronics because of low temperature and low process cost.[1-5] To prevent cross talk between transistors in close proximity and to achieve a low off current in OTFT arrays, it is necessary to pattern the organic semiconductor layer. Several methods have been proposed to pattern organic film, such as evaporating organic film through a shadow mask,[6] depositing a special water-soluble resist on top of the organic semiconductor film followed by lithographic patterning,[7] depositing organic film on the surface with varying surface energies, then using solution dipping to pattern the organic film,[8] and depositing organic film followed by plasma etching and patterning organic film.[9] In our previous works,[8] we found that the substrate surface energy difference between high and low (high/low) surface energy is an important factor affecting the adhesion and the intrusion energy between the pentacene film and the substrate.[8-12] The high/low surface energy difference was controlled by treating with a self-assembly monolayer (SAM) and then exposing to UV light.[8,11] Pentacene growth on the surface with a high/low surface energy difference showed different adhesion characteristics. Using the difference in adhesion and intrusion energy, pentacene patterning was achieved by water dipping.[8]

Instead of developing SAM and UV exposure technology, in this paper a simple approach was first proposed to generate the high/low surface energy difference on dielectric. The proposed method is compatible with conventional photoresist and the photolithography technology. A normal mask can be used to perform the patterning, and the traditional photoresist removal process can also be used.

This work presents a low surface energy material, aluminum nitride (AlN) film, as a substrate surface for pentacene patterning. The AlN film had a low surface energy, so SAM was not needed to lower the surface energy. To pattern the pentacene film on the AlN surface, the AlN high/low surface energy difference was modified by using $O_2$ plasma in this study. Oxygen ($O_2$) and oxygen-containing plasmas are well known to produce a variety of oxygen functional groups and to modify surface energy.[13] After $O_2$ plasma treatment, enlarged surface energy was observed on the AlN surface. From the high/low surface energy difference, this study developed a simple method that can be combined with conventional lithography to pattern pentacene film. The sample was dipped into deionized (DI) water to remove unwanted pentacene film. The chemical bonding environment on the surface of the AlN film modified by $O_2$ plasma was analyzed using X-ray photoelectron spectroscopy (XPS). The XPS data and the calculated intrusion energy supported that the pentacene patterning was governed by the intrusive water between pentacene and the polar functional group on the substrate.

[z] E-mail: hsiaowen@mail.nctu.edu.tw

## Experimental

*Film deposition, patterning, and procedures*.— For pentacene patterning, the surface characteristics of the film were modified using $O_2$ plasma. Figure 1 displays pentacene patterning process flow using the suggested method. As shown in step I, 1000 Å AlN film was deposited on a $n^+$ silicon wafer. The AlN film was deposited at low temperature (150°C) (substrate temperature) using a radio-frequency (rf) sputtering system.[5,14] The silicon wafer was rinsed in DI water, and was then immersed in acetone in an ultrasonic cleaner. The wafer was then dipped in diluted HF solution ($HF:H_2O$ = 1:100) to remove native oxide from the silicon wafer. Finally, the wafer was immediately transferred to the rf-sputtering system. The system was then set to a base pressure of under $2 \times 10^{-6}$ Torr before gas was admitted. Mixed argon and nitrogen gas was monitored by mass flow controllers at an $Ar/N_2$ ratio of 2/9. The AlN film was deposited at a total pressure of 2.5 mTorr. All relevant experimental details have been published elsewhere.[5,14] The AlN film surface was partially capped and defined using conventional photolithography technology in step II. In step III, the sample was transferred to a plasma enhanced chemical vapor deposition (PECVD) system. AlN film surface polarity in the remaining unwanted area was modified using $O_2$ plasma in the PECVD for 10 min. The $O_2$ plasma parameters were rf power 100 W, process pressure 650 mTorr, chamber temperature 100°C, and oxygen gas flow rate 900 sccm. The polarity of the region treated with $O_2$ plasma was changed from hydrophobic to hydrophilic. After the AlN film surface was defined and modified, pentacene film was deposited on the entire surface in step IV. Unpurified Aldrich pentacene material was directly placed in the thermal coater for thermal deposition. The substrate was heated to 70°C during the deposition at a pressure of $3 \times 10^{-6}$ Torr. The thickness of the pentacene film was 100 nm and the deposition rate was 0.5 Å/s, monitored by a quartz crystal oscillator. As shown in step V, to partially lift off and pattern pentacene film, the sample was dipped in DI water. Finally, pentacene patterning on the defined AlN surface was completed.

*Characterization*.— Surface composition and chemical bonding states were investigated using XPS (ESCA PHI1600). X-ray radiation was provided by a monochromated Mg anode Kα line at 1253.6 eV. The base pressure of the instrument was $5 \times 10^{-9}$ Torr. The C 1s at 284.5 eV was used as a reference for all detected peak positions. To separate chemical bonding states in the electron spec-

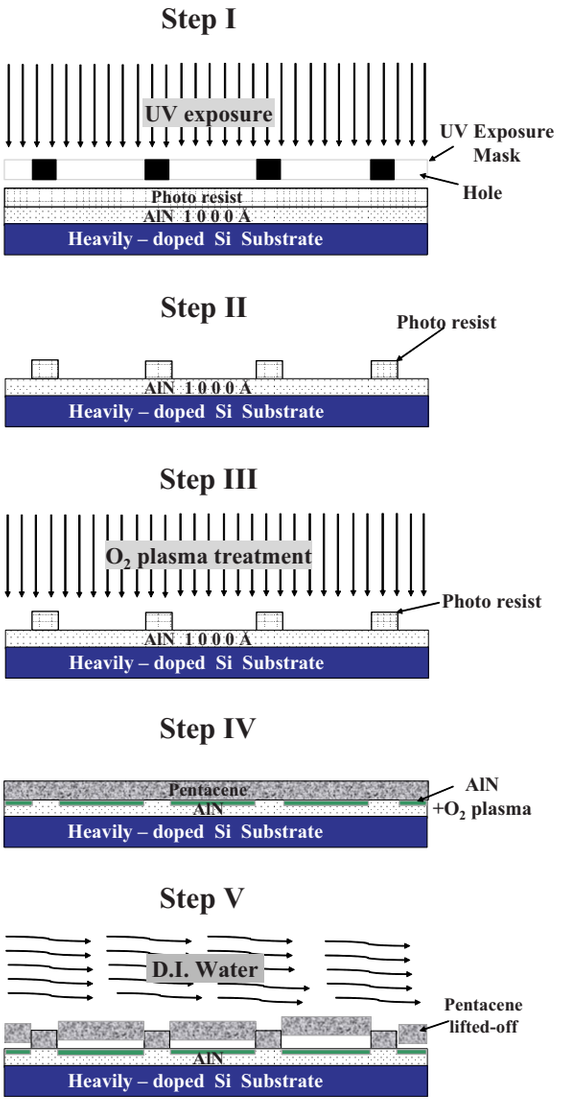


**Figure 1.** (Color online) Schematic showing the proposed pentacene patterning process.

troscopy for chemical analysis (ESCA) spectra, the spectral line shape was simulated using a suitable combination of Gaussian and Lorentzian functions.

The contact angle measurements were used to study migration of hydrophobic and hydrophilic functional groups. The water contact angle was sensitive to film surface chemical composition.[15] The contact angle was obtained by the KRÜSS contact angle system for universal surface testing (model GH-100). Three standard liquids (DI water, diiodo-methane, and ethylene glycol) were applied to measure the contact angles and thus extract the material surface energy. Then, surface energy was calculated using the Fowkes and Young approximation, as in the following equation[16,17]

$$(1 + \cos\theta)\gamma_L = 2(\gamma_S^d\gamma_L^d)^{1/2} + 2(\gamma_S^p\gamma_L^p)^{1/2} \quad [1]$$

where $\theta$ was the measured contact angle; $\gamma_L$ was the tested liquid surface energy and was the sum of its dispersion $\gamma_L^d$ and polar part $\gamma_L^p$; $\gamma_S^d$ and $\gamma_S^p$ were the dispersion and polar components, respectively, of solid surface free energy. The contact angles of three standard liquids (DI water, diiodo-methane, and ethylene glycol) were measured to obtain values of $\gamma_S^d$ and $\gamma_S^p$. The $\gamma_L^d$ and $\gamma_L^p$ values of these standard liquids were used to calculate the $\gamma_S^d$ and $\gamma_S^p$ values of

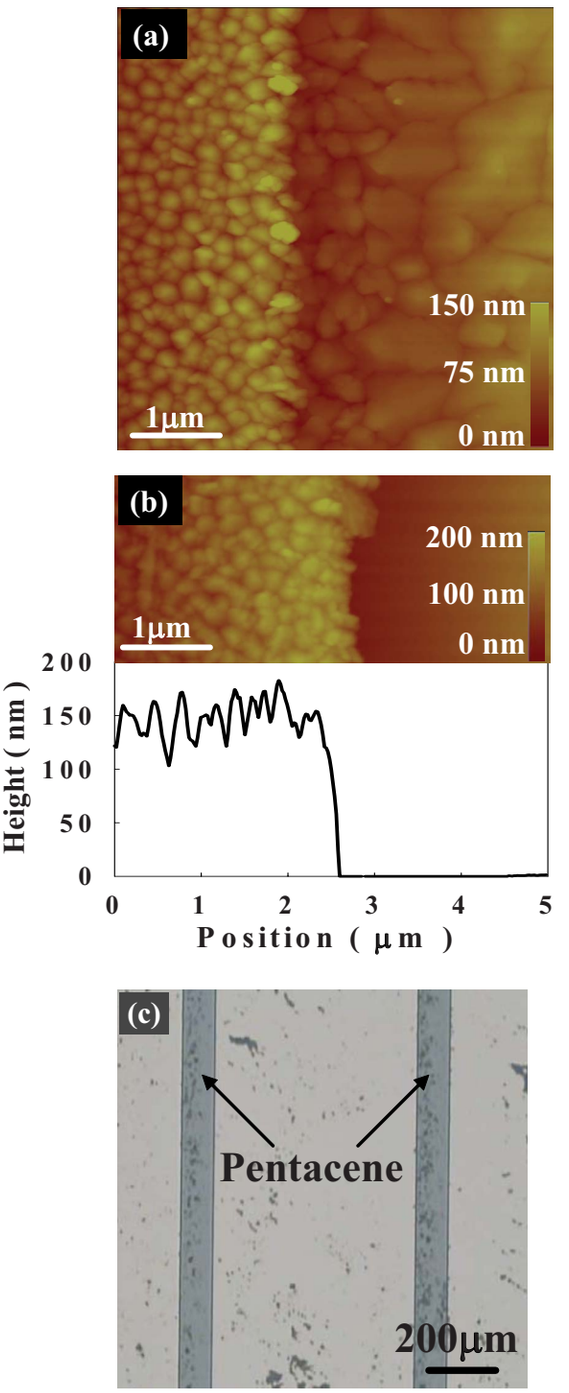


**Figure 2.** (Color online) (a) AFM image showing the pentacene morphology after step IV in Fig. 1. The grain size of pentacene is larger on the AlN treated with $O_2$ plasma. (b) AFM image showing the pentacene morphology after step V in Fig. 1. The pentacene on the AlN treated with $O_2$ plasma is removed by water dipping. The height difference across the pentacene stripe is also shown in (b). The measured height difference is ~150 nm, which is larger than the thickness of the deposited pentacene film. This implies that the pentacene film was completely removed. (c) Optical micrograph image showing the patterned pentacene structure.

the dielectric surface. Also, the total surface free energy of solid $\gamma_S$ was estimated by using

$$\gamma_S \cong \gamma_s^p + \gamma_s^d \quad [2]$$

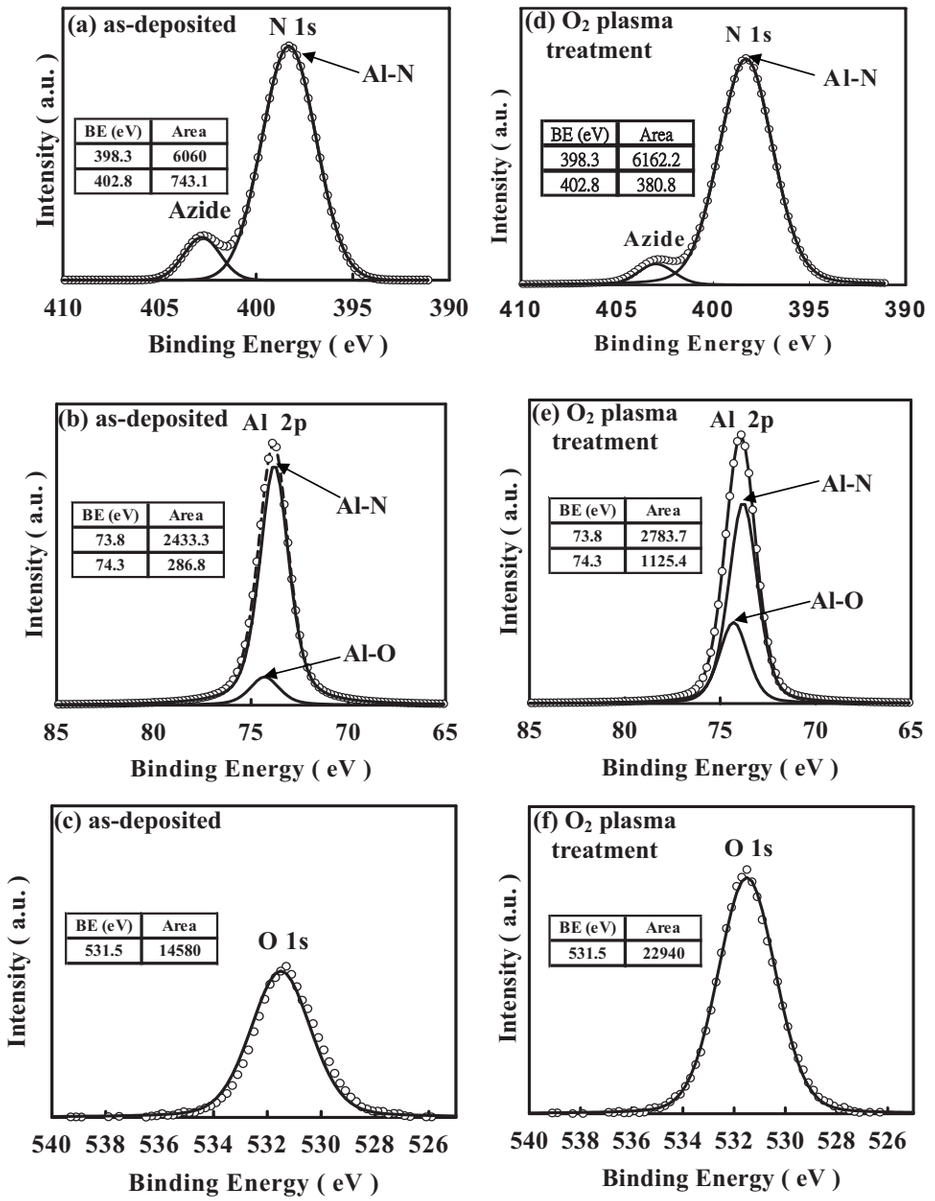


**Figure 3.** XPS spectra of (a) N 1s, (b) Al 2p, and (c) O1s core levels from the as-deposited AlN surface and (d) N 1s, (e) Al 2p, and (f) O1s core levels from the $O_2$ plasma-treated AlN surface. The energy position and peak area of the curve-fit data are listed in the inserted table.

## Results and Discussion

*Pentacene patterning*.— Pentacene patterning was achieved in this study. A pentacene film was deposited on the entire AlN surface which was partially treated with $O_2$ plasma (Fig. 1, step IV). These samples were then dipped in DI water to partially lift off and achieve pentacene patterning. In Fig. 2a, the atomic force microscopic (AFM) image of the pentacene morphology on the border of the region treated with $O_2$ plasma is shown. The surface morphology was measured by using the Digital Instrument AFM model Dimension 3100 tapping mode. The morphology of pentacene depends on whether or not the AlN surface is treated with $O_2$ plasma. Large pentacene grains appear on the $O_2$ plasma-treated region (right), as shown in Fig. 2a.

Differences in surface energy led to different results after dipping in DI water. The pentacene film grown on the $O_2$ plasma-treated region was lifted off after dipping in water. The AFM image in Fig. 2b reveals that, after dipping, the pentacene film on the nontreated area was almost unchanged while that on the $O_2$ plasma-treated area was removed. The height difference of these two areas is approximately 150 nm; this is thicker than the pentacene film thickness (100 nm). This implies that the pentacene film was almost completely removed in this pentacene patterning process. The optical image in Fig. 2c shows two pentacene stripes on the patterned surface. After the proposed pentacene patterning process, the pentacene on the $O_2$ plasma-treated area was clearly removed. The width of a patterned pentacene stripe using the proposed pentacene patterning process was about 100 μm in this study. The pentacene patterning mechanism is attributed to the surface polarity of AlN, which will be characterized and discussed in the following sections.

*Surface chemistry of the AlN film*.— To understand the surface chemistry of AlN film treated with $O_2$ plasma, the AlN surfaces were characterized using XPS. As shown in Fig. 3, XPS spectra of N 1s, Al 2p, and O1s core levels from the AlN surface treated with/without $O_2$ plasma are shown in Fig. 3a-f, respectively. The N 1s core level from the as-deposited AlN surface was approximately 398.3 eV in the binding energy scale as shown in Fig. 3a. A small peak at approximately 402.8 eV next to the N 1s peak was the azide

($N_3^-$) peak.[18] The existence of azide in AlN resulted from the incomplete dissociation of nitrogen in low-power plasma operation conditions. Both N 1s and azide peaks were also observed for the $O_2$ plasma-treated AlN surface as shown in Fig. 3d. The N 1s intensity remains unchanged. However, the azide peak became weaker. This may be due to the reduction of the azide group by gaining electrons from the plasma to the electron-deficient nitrogen. Figure 3b shows the Al 2p core level from the as-deposited AlN surface. The as-deposited AlN surface was partially oxidized because the O 1s signal also appears in the XPS spectrum as shown in Fig. 3c. The partially oxidized AlN surface was expected because the as-deposited AlN surface was exposed to air before the pentacene deposition. The curve-fit data in Fig. 3b indicate that the Al 2p signal consists of an Al–O peak at 74.3 eV and a pure Al–N peak at 73.8 eV.[19] The ratio of Al–O to Al–N increased when the as-deposited AlN surface was treated with $O_2$ plasma for 10 min, as shown in the curve-fit spectra of Al–N and Al–O in Fig. 3e. This was attributed to the oxidation of AlN film near the surface in the $O_2$ plasma bombardment process. $O_2$ plasma oxidation is further confirmed by the increase of O 1s signal, according to the relative peak area of O 1s in Fig. 3c and f. The increase of the ratio of Al–O to Al–N made the AlN surface more polar because the polarity of Al–O was higher than that of Al–N. The AlN surface thus became hydrophilic and increased possible reactions with water. This may have played an important role in the lift-off step using water dipping in pentacene patterning.

*Pentacene morphology.*— After $O_2$ plasma treatment, a pentacene film was evaporated on the AlN surface. Pentacene surface morphology is presented in Fig. 4a and b. The pentacene film on the $O_2$ plasma-treated surface showed large and dendritelike grains. Small grains were observed in pentacene film grown on the untreated AlN surface.

Pentacene growth can be affected by factors such as surface roughness and surface energy. The effect of surface roughness on pentacene growth has been previously reported.[20-25] After $O_2$ plasma treatment, surface roughness was altered from 0.253 to 0.262 as shown in Fig. 4c and d. The change of AlN surface roughness was very small after the $O_2$ plasma treatment. Pentacene growth was considered not affected by surface roughness in our study. Yang et al. proposed that pentacene grain morphology was affected by surface energy.[26] As shown in Fig. 4c and d insets, the water contact angle decreased from 81.7 to 3.3° after $O_2$ plasma treatment. The relative surface energy was derived from the water contact angles using Eq. 1 and 2, and listed in Table I. The polar and dispersive components of the surface energy were also derived and listed in Table I. The surface energy increases after $O_2$ plasma treatment. Note that large grains of pentacene growth on a surface with large surface energy were observed. The increase of pentacene grain size on the plasma-treated AlN surface is thus attributed to an increase in surface energy.

*Pentacene patterning analyses.*— To identify the pentacene patterning mechanism, adhesion energy was used to characterize the adhesive strength of pentacene to different surfaces. The adhesion energy between materials, given by the following equations, has been presented elsewhere[8,27,28]

$$E_{\text{before}} = 2\left(\sqrt{\gamma_{\text{pe}}^{\text{p}}\gamma_{\text{s}}^{\text{p}}} + \sqrt{\gamma_{\text{pe}}^{\text{d}}\gamma_{\text{s}}^{\text{d}}}\right) \quad [3]$$

where $E_{\text{before}}$ denotes the adhesion energy between pentacene and the substrate before dipping in water; $\gamma_{\text{pe}}^{\text{p}}$ and $\gamma_{\text{pe}}^{\text{d}}$ are the polar and the dispersion components of the pentacene surface energy, and $\gamma_{\text{s}}^{\text{p}}$ and $\gamma_{\text{s}}^{\text{d}}$ are the polar and the disperse components of the substrate surface energy, respectively. The calculated adhesion energy is summarized in Table II. The adhesion energy $E_{\text{before}}$ between the pentacene film and the $O_2$ plasma-treated AlN surface is larger than the untreated surface. The increase in adhesion energy is not consistent with water-removable characteristics. Generally, higher adhesion is achieved when an organic film is deposited on a higher polar substrate.[29] The Al 2p XPS spectra presented in Fig. 3b and e and the O 1s spectra in Fig. 3c and f can be used to explain the higher adhesion energy. The higher polar surface was obtained according to the enhanced Al–O bonding signal after $O_2$ plasma treatment. These results were consistent with the higher polar component of surface energy after $O_2$ plasma treatment as listed in Table I.

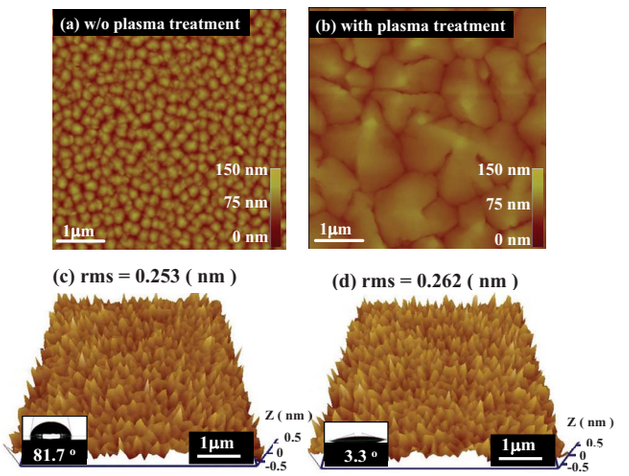


**Figure 4.** (Color online) AFM images showing pentacene on (a) the as-deposited AlN surface and on (b) the $O_2$ plasma-treated AlN surface. The AFM images of surface roughness of (c) the as-deposited AlN surface and (d) the $O_2$ plasma-treated AlN surface. The corresponding optical micrograph of the water contact angle on the AlN surface is inserted in the lower-left corner. The surface height is expressed on the *z*-axis scale. The surface height is expressed by the relative contrast in the AFM images.

Intrusion energy $E_{\text{I}}$ was calculated to confirm the water-removable characteristics. Intrusion energy is caused by the interaction of water, pentacene, and the AlN surface. The adhesion energy is affected by the intrusion energy $E_{\text{I}}$ according to the equation

$$E_{\text{after}} = E_{\text{before}} - E_{\text{I}} \quad [4]$$

where $E_{\text{after}}$ denotes the adhesion energy after dipping in water. The intrusion energy $E_{\text{I}}$ is calculated using the following equation

$$E_{\text{I}} = 2\{\sqrt{\gamma_{\text{so}}^{\text{p}}\gamma_{\text{s}}^{\text{p}}} + \sqrt{\gamma_{\text{so}}^{\text{d}}\gamma_{\text{s}}^{\text{d}}} + \sqrt{\gamma_{\text{pe}}^{\text{p}}\gamma_{\text{so}}^{\text{p}}} + \sqrt{\gamma_{\text{pe}}^{\text{d}}\gamma_{\text{so}}^{\text{d}}} - [\gamma_{\text{so}}^{\text{p}} + \gamma_{\text{so}}^{\text{d}}]\} \quad [5]$$

where $\gamma_{\text{so}}^{\text{p}}$ and $\gamma_{\text{so}}^{\text{d}}$ are the polar and disperse components of the surface energy of the dipping solution (DI water), respectively. Table II lists the calculated intrusion energy $E_{\text{I}}$ and the adhesion energy after dipping in water, i.e., $E_{\text{after}}$. $E_{\text{I}}$ increases significantly after the $O_2$ plasma treatment. Consequently, $E_{\text{after}}$ decreases to less than zero after the $O_2$ plasma treatment. Specifically, the $E_{\text{after}}$ of the untreated region is 51.5 mJ/m$^2$ and that of the treated region is −38.5 mJ/m$^2$. This fact explains the experimental results in Fig. 2b. The pentacene on the untreated area was almost unaffected because $E_{\text{after}}$ was large; the pentacene film on the area that had been treated by $O_2$ plasma was removed by dipping in water because $E_{\text{after}}$ became negative. Also, the large difference between the $E_{\text{after}}$ of the

**Table I. Water contact angles and the corresponding surface energies of the as-deposited AlN surface and the $O_2$ plasma-treated AlN surface.**

| | Without $O_2$ plasma treatment | With $O_2$ plasma treatment |
|---|---|---|
| Water contact angle (degree) | 81.7 | 3.3 |
| Surface energy $\gamma_s$ (mJ/m$^2$) | 53 | 161.2 |
| Polar component $\gamma_S^p$ (mJ/m$^2$) | 13.2 | 114.4 |
| Disperse component $\gamma_S^d$ (mJ/m$^2$) | 39.8 | 46.8 |

**Table II. Intrusion energy and adhesion energy between the pentacene film and the AlN surface in various experimental conditions.**

| | Without $O_2$ plasma treatment | With $O_2$ plasma treatment |
|---|---|---|
| Adhesion energy $E_{before}$ (mJ/m$^2$) | 86.1 | 101.9 |
| Intrusion energy $E_I$ (mJ/m$^2$) | 34.5 | 140.4 |
| Adhesion energy $E_{after}$ (mJ/m$^2$) | 51.5 | −38.5 |

untreated area and that of the treated area completely explains pentacene patterning capacity.

Higher polar surfaces can more easily react with polar solutions, which have been reported in previous studies.[10,30,31] The interface of the pentacene film and a higher polar AlN surface reacts more easily with DI water during water dipping. This result was consistent with the higher intrusion energy (140 mJ/m$^2$) on the $O_2$ plasma-treated surface when the interface was dipped in DI water. The high intrusion energy associated with high polar surface energy of the $O_2$ plasma-treated AlN surface explained the water-removable pentacene patterning mechanism.

## Conclusion

A simple pentacene patterning process has been developed using water dipping. The pentacene was completely lifted off by water dipping on the area of AlN treated with $O_2$ plasma. The AlN surface treated with $O_2$ plasma becomes more polar after the $O_2$ plasma treatment based on surface energy measurements. The polar surface energy enhanced the intrusion energy of water and helped lift off the pentacene film on the $O_2$ plasma-treated AlN surface. The high intrusion energy associated with the high polar surface energy of the $O_2$ plasma-treated AlN surface explained the water-removable pentacene patterning mechanism. The simple pentacene patterning process is compatible with conventional lithography and is applicable to future OTFT array processes.

## Acknowledgments

The authors thank H. T. Song at Display Institute, National Chiao Tung University and Wei-Yu Chen at the Materials Science and Engineering Institute, National Tsing Hua University for their support on film deposition and ESCA measurement. This work was funded through the National Science Council of Taiwan (contract no. NSC 96-2221-E-009-127-MY2) and AU Optronics Corporation. The authors also are thankful for the experimental support from National Nano Device Laboratories.

*National Chiao Tung University assisted in meeting the publication costs of this article.*

## References

1. K. Nomoto, N. Hirai, N. Yoneya, N. Kawashima, M. Noda, M. Wada, and J. Kasahara, *IEEE Trans. Electron Devices*, **52**, 1519 (2005).
2. Q. Cao, Z.-T. Zhu, M. G. Lemaitre, and M.-G. Xia, *Appl. Phys. Lett.*, **88**, 113511 (2006).
3. S. F. Nelson, Y.-Y. Lin, D. J. Gundlach, and T. N. Jackson, *Appl. Phys. Lett.*, **72**, 1854 (1998).
4. C. Goldmann, S. Haas, C. Krellner, K. P. Pernstich, D. J. Gundlach, and B. Batlogg, *J. Appl. Phys.*, **96**, 2080 (2004).
5. H.-W. Zan, K.-H. Yen, P.-K. Liu, K.-H. Ku, C.-H. Chen, and J. Hwang, *Jpn. J. Appl. Phys., Part 2*, **45**, L1093 (2006).
6. P. F. Baude, D. A. Ender, M. A. Haase, T. W. Kelly, D. V. Mures, and S. D. Theiss, *Appl. Phys. Lett.*, **82**, 22 (2003).
7. M. G. Kane, J. Campi, M. S. Hammond, B. Greening, C. D. Sheraw, J. A. Nichols, D. J. Gundlach, J. R. Huang, C. C. Kuo, L. Jia, et al., *IEEE Electron Device Lett.*, **21**, 11 (2000).
8. H. W. Zan, C. W. Chou, and K. H. Yen, *Thin Solid Films*, **516**, 2231 (2008).
9. S. H. Kim, H. Y. Choi, S. H. Han, J. H. Hur, and J. Jang, in *SID2004 Symposium Proceedings 45.2*, p. 1297 Society for Information Display 2004, San Jose, CA, May 25–27 (2004).
10. C. M. Chan, *Polymer Surface Modification and Characterization*, Ch. 6, p. 237, Hanser Gardner, New York (1994).
11. M. Ando, M. Kawasaki, S. Imazeki, H. Sasaki, and T. Kamata, *Appl. Phys. Lett.*, **85**, 1849 (2004).
12. D. R. Hines, S. Mezhenny, M. Breban, and E. D. Williams, *Appl. Phys. Lett.*, **86**, 163101 (2005).
13. H. Y. Yu, X. D. Feng, D. Grozea, Z. H. Lu, R. N. S. Sodhi, A.-M. Hor, and H. Aziz, *Appl. Phys. Lett.*, **78**, 2595 (2001).
14. C.-M. Yeh, C. H. Chen, J.-Y. Gan, C. S. Kou, and J. Hwang, *Thin Solid Films*, **483**, 6 (2005).
15. C. M. Chan, *Polymer Surface Modification and Characterization*, Ch. 2, p. 35, Hanser Gardner, New York (1994).
16. D. Myers, *Surfaces, Interfaces, and Colloids: Principles and Applications*, 2nd ed., p. 430, John Wiley & Sons, New York (1999).
17. F. M. Fowkes, *J. Phys. Chem.*, **67**, 2538 (1963).
18. D. C. Boyd, R. T. Haasch, D. R. Mantell, R. K. Schulze, J. F. Evans, and W. L. Gladfelter, *Chem. Mater.*, **1**, 119 (1989).
19. J. A. Kovacich, J. Kasperkiewicz, D. Lichtman, and C. R. Aita, *J. Appl. Phys.*, **55**, 2935 (1984).
20. K. Shin, S. Y. Yang, C. Yang, H. Jeon, and C. E. Park, *Org. Electron.*, **8**, 336 (2007).
21. D. Knipp, R. A. Street, and A. R. Völkel, *Appl. Phys. Lett.*, **82**, 3907 (2003).
22. D. Knipp, R. A. Street, A. R. Völkel, and J. Ho, *J. Appl. Phys.*, **93**, 347 (2003).
23. S. Steudel, S. D. Vusser, S. D. Jonge, D. Janssen, S. Verlaak, J. Genoe, and P. Heremans, *Appl. Phys. Lett.*, **85**, 4400 (2004).
24. S. E. Fritz, T. W. Kelley, and C. D. Frisbie, *J. Phys. Chem. B*, **109**, 10574 (2005).
25. K. Shin, C. Yang, S. Y. Yang, H. Jean, and C. E. Park, *Appl. Phys. Lett.*, **88**, 072109 (2006).
26. S. Y. Yang, K. Shin, and C. E. Park, *Adv. Mater. (Weinheim, Ger.)*, **15**, 1806 (2005).
27. H. Nagata and A. Kawai, *Jpn. J. Appl. Phys., Part 1*, **28**, 2137 (1989).
28. D. H. Kaelble, *J. Appl. Polym. Sci.*, **18**, 1869 (1974).
29. C. M. Chan, *Polymer Surface Modification and Characterization*, Ch. 6, p. 261, Hanser Gardner, New York (1994).
30. C. J. Huang and W. C. Shih, *J. Electron. Mater.*, **32**, 478 (2003).
31. C. C. Yeh, Y. J. Lin, S. K. Lin, Y. H. Wang, S. F. Chung, L. M. Huang, and T. C. Wen, *J. Vac. Sci. Technol. B*, **25**, 1635 (2007).